# Langevin molecular dynamics with quantum forces: Application to silicon clusters

N. Binggeli
*Institut Romand de Recherche Numérique en Physique des Matériaux (IRRMA), PHB Ecublens, 1015 Lausanne, Switzerland*

James R. Chelikowsky
*Department of Chemical Engineering and Materials Science, Minnesota Supercomputer Institute, University of Minnesota, Minneapolis, Minnesota 55455*

(Received 17 June 1994)

We have implemented a dynamical stochastic scheme to determine from first principles the structure of complex low-symmetry atomic systems such as surfaces and clusters. The method is based on Langevin molecular dynamics and quantum-mechanical interactions derived from *ab initio* pseudopotential calculations. No fictitious electron dynamics is employed, and insulating as well as metallic or charged systems can be handled in a straightforward manner. We apply this method together with the simulated annealing strategy to small neutral and charged silicon clusters, and show that the ground-state structures can be efficiently obtained with this approach. We also exploit this scheme to perform first-principles isothermal molecular-dynamics simulations, and examine the adsorption of a Si atom on a cluster.

## I. INTRODUCTION

The structural determination of complex, nonperiodic systems is one of the outstanding problems in materials science. Traditional theoretical approaches are hindered by the large number of degrees of freedom, and the lack of symmetry in these systems. Consider determining the structure of a cluster. For very small clusters it may be possible to create an exhaustive inventory of topologically distinct structures, and examine the total energy of each structure. In this way, one may examine all possible structures, and obtain the "true" ground state. However, once the cluster size exceeds a half dozen atoms or so, it becomes virtually impossible to construct such an inventory, and to do computations on all the possibilities. Computer simulations which exploit a simulated annealing strategy[1] can help overcome some of these obstacles. These computer "experiments" are not prejudiced by preconceived notions of the structure topology. The challenge with such extensive numerical investigation is to reconcile an accurate description of the potential-energy surface with a comprehensive exploration of the configuration space to achieve a global geometry optimization.

A number of simulation techniques have been exploited to perform simulated annealing. Most of the schemes were coupled to empirical descriptions of the interatomic potentials. One such scheme is the Monte Carlo (MC) approach.[1] This is a robust scheme that is well suited for complex energy surfaces. Only the energy needs to be computed in the MC approach; this approach does not require interatomic forces. However, in general, MC is not the most efficient approach. Information on forces is not used, so the simulation can waste time exploring high-energy configurations. In addition, MC may be difficult to implement in terms of constructing a vectorizable computing algorithm.

Traditional Newtonian molecular dynamics (MD) is more efficient than the MC scheme when the energy surface is smooth, but MD is likely to be affected by the existence of local minima in complex energy surfaces. Biswas and Hamann[2] have proposed a procedure which combines some of the advantages of MC with MD. Namely, they implemented a Langevin molecular dynamics (LMD) for simulated annealing. The LMD introduces a stochastic element into the Newtonian dynamics. The stochastic nature of the LMD allows energetically unfavorable configurations to be sampled, and can avoid the trapping of clusters in metastable states. On the other hand, LMD takes into account information from the interatomic forces. With an empirical force field description, this approach has been applied to clusters[2–4] with some success.

Classical force fields offer many advantages over first-principles quantum calculations in the study of the structure and properties of matter containing more than a few atoms. Such fields are well known in the study of interactions of closed-shell atoms in terms of central forces, such as van der Waals interactions. However, open-shell atoms may interact through mixtures of central two-body and directional, or many-body, forces. Such many-body forces are very difficult to replicate with force fields. Essentially, one is attempting to transcribe "quantum forces" into "classical forces." Quantum forces which involve coordination changes, rehybridization, and Jahn-Teller distortions have no simple classical analog. To handle such issues, one would like to replace the empirical interatomic potentials with the "real" quantum forces. Until recently, this replacement appeared to be impossible. The time requires for quantum force calculations can be several orders of magnitude longer, at a minimum, than the time required for classical forces.

0163-1829/94/50(16)/11764(7)/$06.00  

We illustrate that it is possible to combine LMD with quantum forces. The forces are determined from *ab initio* pseudopotentials constructed within the local-density approximation. Our approach differs from that of Car and Parrinello[5] who incorporated pseudopotentials within a molecular-dynamics framework. Their approach can be applied to complex systems and has been used to examine small clusters.[6–11] The Car-Parrinello method uses *fictitious* dynamics for the electrons and *Newtonian dynamics* for the ions, simultaneously minimizing the energy with respect to the electronic and ionic degrees of freedom. However, it is not necessary to employ fictitious electron dynamics to achieve an efficient simulation procedure.[12–14]

In the approach presented here, we do not use fictitious electron dynamics. We constrain the system to the Born-Oppenheimer surface. This constraint requires a self-consistent solution for each time step of the simulation, but the time steps used in this procedure can be one to two orders of magnitude larger than with the Car-Parrinello method.[15] Our procedure is also more straightforward to implement for metallic systems. We would like to stress that the Langevin dynamics used here is a proper scheme to generate a *canonical ensemble.* It can be exploited to perform *isothermal molecular-dynamics simulations* as well as simulated annealing.

As an illustrative application of the method, we examine silicon clusters. Specifically, we will study several clusters of $Si_n$ with $n \leq 13$. We determine the ground state of neutral and charged species of these clusters, and exploit the Langevin constant-temperature scheme to examine a simple adsorption process. Si clusters present obstacles to an accurate theoretical description. Angular forces are important, and can vary significantly from one coordination state to another. Our experience with semiconductor surfaces, which is confirmed by previous work on silicon clusters, suggests that small clusters can undergo large reconstructions, and do not resemble fragments of crystalline silicon.

Experimental data on silicon clusters have suggested a complex structural and electronic behavior. The reactivity of silicon clusters with gas-phase molecular reagents can vary strongly according to the cluster size. For example, $Si_{13}^+$ is much less reactive than other clusters when exposed to oxygen, ammonia, ethylene, or water.[16] This low reactivity to a variety of different species suggests that the $S_{13}^+$ cluster may possess a special geometry. In fact, interatomic potentials for neutral species have suggested that silicon clusters exhibit an icosahedral growth pattern with $Si_{13}$ and $Si_{19}$ being special structures.[3] Moreover, silicon clusters as a function of size have very different mobilities.[16] Small clusters $Si_n$, $n \lesssim 25$ exhibit a uniaxial growth pattern, whereas for $n \gtrsim 25$, the growth pattern suggests a more spheroidal geometry. This morphological transformation is also compatible with the growth patterns suggested by interatomic potentials. However, the structures suggested by interatomic potentials are not in accord with quantum calculations. "Quantum" Langevin molecular dynamics (QLMD) can provide insights into such issues. We can explore a variety of morphologies without prejudice toward any particular model.

## II. COMPUTATIONAL METHODS

In our simulations, the ionic positions, $\mathbf{R}_j$ evolve according to the Langevin equation:

$$M_j\ddot{\mathbf{R}}_j = -\nabla_{\mathbf{R}_j} E(\{\mathbf{R}_i\}) - \gamma \mathbf{M}_j \dot{\mathbf{R}}_j + \mathbf{G}_j \ , \tag{1}$$

where $E(\{\mathbf{R}_i\})$ is the total energy of the system and $\{M_i\}$ are the ionic masses. The last two terms on the right-hand side of Eq. (1) are the dissipation and fluctuation forces, respectively. The dissipative forces are defined by the friction coefficient $\gamma$. The fluctuation forces are defined by random Gaussian variables $\{\mathbf{G}_j\}$, with a white spectrum:

$$\begin{aligned} &\langle G_i^\alpha(t)\rangle = 0 \ , \\ &\langle G_i^\alpha(t) G_j^\alpha(t')\rangle = 2\gamma M_i k_B T \delta_{ij} \delta(t-t') \ . \end{aligned} \tag{2}$$

The angular brackets denote ensemble or time averages, and $\alpha$ stands for the Cartesian component. The coefficient on the right-hand side of Eq. (2) insures that the fluctuation-dissipation theorem is obeyed.[17,18]

For a system with natural or periodic boundary conditions, it can be shown (see the Appendix) that the canonical distribution

$$P_0 \sim \exp\left[ -\frac{\sum_j \frac{1}{2} M_j |\dot{\mathbf{R}}_j|^2 + E(\{\mathbf{R}_i\})}{k_B T} \right] \tag{3}$$

is a steady-state equilibrium solution of the probability distribution associated with the equations of motion (1) and (2).[19] Langevin dynamics can therefore be used as an alternate to Nosé dynamics[20] to perform constant-temperature simulations. In contrast to Nosé dynamics the LMD based on Eqs. (1) and (2) includes a physical heat exchange process which occurs through "collisions and friction" of the particles with the heat bath. The random forces establish the temperature of the system from the fluctuation-dissipation theorem. The presence of a physical viscous medium makes the LMD approach particularly well suited for simulating a cluster in a buffer gas.

The LMD coupled to the simulated annealing procedure can provide a general tool for complex structural optimization. The temperature can be controlled without rescaling the velocities, as is often done in Newtonian MD. Energy can exchange into and out of the system as required by the temperature of the heat bath. Simulated annealing need not follow each time step of the "natural evolution" of the physical system. Annealing rates can be faster if the dynamics lead to acceptable "shortcuts" relative to the natural evolution. As opposed to MC simulations, LMD and MD simulations sample the configuration space by collectively moving the particles. LMD and MD simulations also move faster to the minima in a potential-energy surface by exploiting the interatomic forces. On the other hand, the stochastic nature of

the random forces present in LMD helps the system to escape from metastable states in a manner reminiscent of "uphill" moves in MC simulations.

The interatomic forces $-\nabla_{\mathbf{R}_j} E(\{\mathbf{R}_i\})$ in Eq. (1) are determined quantum mechanically within the local-density approximation to density-functional theory. We use pseudopotentials with a plane-wave basis in a supercell configuration. Provided the supercell is large, interactions between neighboring cells are minimized, and the solutions of the Kohn-Sham equations represent those of an isolated cluster. Unfortunately, this procedure can result in a large plane-wave basis. We use a fast iterative diagonalization procedure[21] and exploit a Broyden mixing scheme[22] to accelerate the convergence of the self-consistent field. At each step in integrating the equation of motions, we determine the self-consistent field. We use the difference between the self-consistent charge density and the superposition of atomic charge densities at each step to extrapolate the charge density at the next step.

In determining the charge density, metallic states are conveniently handled by means of the Gaussian broadening scheme.[23–25] This technique allows us to treat clusters having occupied and empty orbitals which are quasidegenerate, and also properly sample metallic configurations which may occur in a cluster at $T>0$. For charged clusters, the broadening method can be exploited to include a partially occupied electronic orbital. The neutrality of the supercell is maintained in this case by introducing a compensating jellium background.[26]

The *ab initio* pseudopotential for silicon has been optimized for use with a plane-wave basis. This potential was generated using the method of Troullier and Martins.[27] The potential, based on the atomic ground state, as $3s^2 3p^2 3d^0$, was cast into the Kleinman-Bylander separable form[28] with $s$ and $d$ nonlocality. We checked that this potential accurately reproduced the structural and elastic properties of crystalline silicon.

With respect to other technical details, we used the exchange-correlation functional by Ceperley and Alder[29] in the parameterized form given by Perdew and Zunger.[30] The plane-wave cutoff in the basis was taken to be 7 Ry. We used a simple cubic supercell with edge $a=18$ a.u. for the smallest clusters ($n\leq 6$). We tested these parameters by using a cell with double volume and an energy cutoff of 12 Ry. Changes in the structural parameters were less than 1%. For $Si_7$ and $Si_{13}$ we used cubic supercells of dimension $a=20$ and 25 a.u., respectively. We sampled the charge with the $\Gamma$ point, and a Gaussian broadening of $1.5\times 10^{-2}$ Ry was used in determining the state occupation.

With respect to the parameters in Eq. (1), we used a Langevin friction parameter $\gamma=5\times 10^{-4}$ a.u. To integrate the equations of motion (1), we used a modified Beeman integration procedure[31] with a times step of 330 a.u., or 8 fs. For our simulated ground-state search of $Si_n$ clusters, we heated a fragment of crystalline Si, a random structure or a structure resulting from an earlier faster annealing, up to 3000–3500 K, and cooled it to 300 K with six to eight temperature regimes (depending on the cluster size). The annealing schedule was approximately linear and about 100 integration steps were used for each temperature regime. The initial temperatures, 3000–3500 K, were far above the melting point of silicon ($\sim$1750 K) and allowed the simulation to proceed from a weakly interacting state.

## III. THE STRUCTURE OF SILICON CLUSTERS

The ground-state structures for the $Si_n$, $n\leq 7$, clusters are presented in Fig. 1. We present the bond lengths and angles in this figure, and compare to Hartree-Fock calculations[32,33] which include correlation effects via perturbation theory. The resulting ground-state structure of our calculations is in very good agreement with the Hartree-Fock work. The largest error concerns the second-neighbor distance for the $Si_5$ cluster, which is underestimated by 6%. Inspection of the structure of the small clusters, in Fig. 1, shows that their growth can be related to the adsorption of new atoms at appropriate edge-capping or face-capping locations, followed by relatively minor distortions of the overall cluster structure.

For these small clusters, it is relatively straightforward to determine the ground-state structure. However, even for a cluster as small as $Si_6$, issues can arise as to the "true" ground state. A typical annealing for $Si_6$ is shown in Fig. 2. The initial random geometry, the final struc-

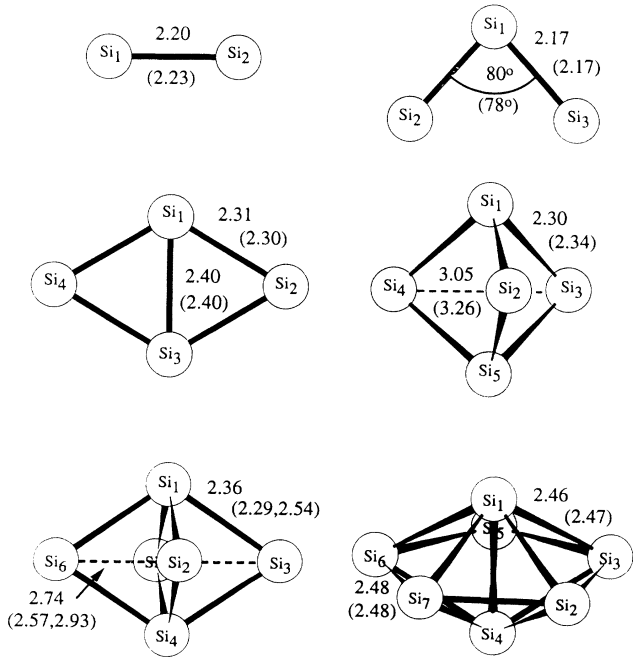


FIG. 1. LDA ground-state geometry of the neutral $Si_2$–$Si_7$ clusters. The bond lengths are in Å. The results from the Hartree-Fock calculations (Refs. 32 and 33) are given in parentheses. The corresponding bond angles are $\theta_{1\text{-}2\text{-}3}=63°$ (63°) for $Si_4$, $\theta_{1\text{-}3\text{-}5}=80°$ (73°) and $\theta_{2\text{-}1\text{-}3}=83°$ (88°) for $Si_5$, $\theta_{1\text{-}3\text{-}4}=70°$ (75°,71°) and $\theta_{2\text{-}1\text{-}3}=71°$ (68°,70°) for $Si_6$, and $\theta_{1\text{-}3\text{-}4}=62°$ (63°) and $\theta_{2\text{-}1\text{-}3}=60°$ (60°) for $Si_7$.

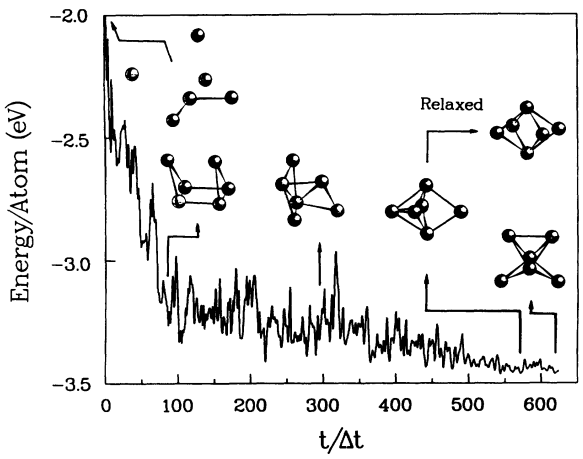


FIG. 2. Binding energy of $Si_6$ during a typical Langevin annealing run from 3000 to 300 K. The time step $\Delta t$ is $8\times10^{-15}$ sec. The initial, final, and some of the intermediate configurations of the cluster are shown. Bonds are drawn for interatomic distances smaller than 2.60 Å.

ture, and a few representative examples of the structures occurring during the anneal are illustrated in this figure. During the annealing process, we can examine possible high-temperature structures. For example, in the early stages of the anneal, a triangular prism structure occurs. This structure has been found to be a structural unit for several clusters with $n > 8$. We find as lowest-energy structures two isomers which are quasidegenerate within the accuracy of the calculation. These structures are a bicapped tetrahedron and an edge-capped trigonal bipyramid which subsequently relaxes to a distorted octahedron (Fig. 2). Hartree-Fock calculations yield binding energies for these two structures which are also within 0.01 eV/atom. In Fig. 1, for simplicity, we represented only the distorted octahedron.

We examined the negatively charged clusters $Si_n^-$ with $n \leq 7$, and found structures similar to those of the neutral clusters (Fig. 1). Optimized structural parameters for these clusters are given in Table I together with the corresponding Hartree-Fock results.[34] The bond lengths are in excellent agreement with the Hartree-Fock results. A typical bond-length difference from the Hartree-Fock work is on the order of $\sim$0.03 Å. We have also done some calculations for the positively charged clusters, e.g., $Si_6^+$, using the same annealing procedure as for the neutral cluster. In the case of $Si_6^+$, we do find some structural changes from the neutral cluster. Namely, we find the edge-capped trigonal bipyramid as the final structure of the annealing process.

In Fig. 3, we show the lowest-energy structure obtained for $Si_{13}$. The structure can be described as a capped "antiprism." This structure is consistent with the result of other LDA calculations.[11] We found some other minima from the annealings corresponding to somewhat different structures. These structures differed from the structure shown in Fig. 3 by some local distortions and some bond switchings. Such structures were about 0.03 to 0.05 eV/atom higher in energy than the structure shown in Fig. 3. The relaxed icosahedral structure, instead, is about 0.2 eV/atom higher in energy than the capped antiprism.

The ideal icosahedral structure for $Si_{13}$ is unstable against Jahn-Teller distortions. One possible issue which has not been investigated theoretically is the effect of charging the $Si_{13}$ cluster. This may be an important consideration as the reactivity studies have been performed on $Si_{13}^+$ clusters and not on the neutral species. The ideal icosahedral $Si_{13}$ structure possesses a fourfold-degenerate highest-occupied orbital populated by two electrons. Removing an electron from the neutral $Si_{13}$

TABLE I. LDA bond lengths (in Å) and angles for $Si_2^-$–$Si_7^-$. The bonds are labeled according to Fig. 1. The results of the Hartree-Fock (HF) calculations (Ref. 34) are also given.

| | Bond (angle) | LDA | HF |
|---|---|---|---|
| $Si_2^-(\Pi_u)$ | $d_{1,2}$ | 2.15 | 2.20 |
| $Si_3^-(B_2)$ | $d_{1,2}$ | 2.29 | 2.32 |
| | $\theta_{2\text{-}1\text{-}3}$ | 59° | 57° |
| $Si_4^-$ | $d_{1,2}$ | 2.31 | 2.32 |
| | $d_{1,3}$ | 2.35 | 2.37 |
| | $\theta_{1\text{-}2\text{-}3}$ | 61° | 61° |
| $Si_5^-$ | $d_{1,2}$ | 2.32 | 2.34 |
| | $d_{2,3}$ | 2.70 | 2.75 |
| | $\theta_{1\text{-}3\text{-}5}$ | 96° | 95° |
| | $\theta_{2\text{-}1\text{-}3}$ | 71° | 72° |
| $Si_6^-$ | $d_{1,2}$ | 2.41 | 2.41 |
| | $d_{2,3}$ | 2.59 | 2.56 |
| | $\theta_{1\text{-}3\text{-}4}$ | 81° | 83° |
| | $\theta_{2\text{-}1\text{-}3}$ | 65° | 64° |
| $Si_7^-$ | $d_{1,2}$ | 2.53 | 2.54 |
| | $d_{2,3}$ | 2.45 | 2.42 |
| | $\theta_{1\text{-}3\text{-}4}$ | 69° | 72° |
| | $\theta_{2\text{-}1\text{-}3}$ | 58° | 57° |

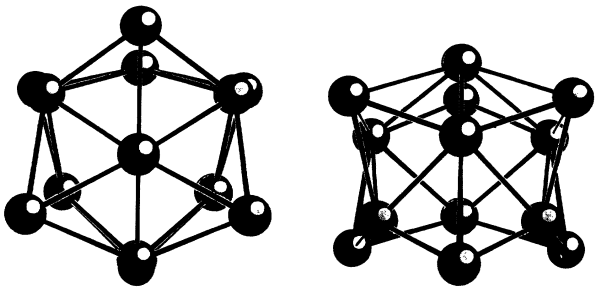

FIG. 3. Low-energy structure for $Si_{13}$. This structure can be seen as a capped "antiprism." Top and side views of the structure are illustrated.

cluster stabilizes somewhat the icosahedral structure against the Jahn-Teller distortion. The energy difference between the icosahedral type and the antiprism type of structure decreases to about 0.1 eV/atom.

Within the LDA framework, several isomers for $Si_{13}$ are within a few $k_B T$, at the experimental temperature. Under these conditions, dynamical stabilization effects or effects beyond the LDA (Ref. 35) may play a critical role in determining the most probable structure. Understanding the low reactivity of $Si_{13}$ and its relationship to the icosahedral structure are still somewhat problematic.[35] We believe further experimental and theoretical analyses will be necessary to settle such issues. For instance, theoretical and experimental photoelectron or Raman spectra[36] may be very useful to identify the relevant structures. Although, to our knowledge, no experimental photoelectron spectra are yet available for $Si_{13}$, we are presently investigating the electronic spectra of the clusters at finite temperature.

## IV. ADSORPTION OF A SILICON ATOM

The growth of the small clusters can be depicted as the result of an edge capping or face capping of a smaller cluster ($Si_{n-1}$ or a magic number cluster), followed by relatively minor distortions of the overall structure. Therefore, it may be useful to investigate a growth process by sequential addition of atoms. This approach may help the search for low-energy structures of the clusters.

We have studied the binding of an adatom to the $Si_7$ cluster by means of Langevin constant-temperature simulations. For these simulations, we used a 25-a.u. cubic cell and positioned the Si atom 10 a.u. away from the surface of the cluster. We generated starting configurations with the Si atom at various angles from the cluster. The simulations were carried out at two different temperatures: 1500 and 2000 K. The isothermal simulations proceeded for about 1.5 ps. During this time the adatom could bind to the cluster and the new system evolve isothermally for $\sim 0.5$ to 1 ps. The structure was then quenched to 300 K in $\sim 1-2$ ps.

Snapshots of typical configurations occurring during a simulation at 2000 K are presented in Fig. 4. The initial configuration is shown in Fig. 4(a). The adatom binds to a single atom of the cluster [Fig. 4(b)], and then moves to edge-capped locations [Fig. 4(c)]. The simulation then samples some face-capped configurations [Fig. 4(d)]. The structure resulting from the annealings after the isothermal simulations at 2000 K was the bicapped octahedron shown in Fig. 4(e). The latter structure coincides with the stable form of $Si_8$.[7,33] At 1500 K, the annealed structures were either an edge-capped $Si_7$ type of structure or a bicapped-octahedron type of structure. The latter geometries included the ground-state structure shown in Fig. 4(e).

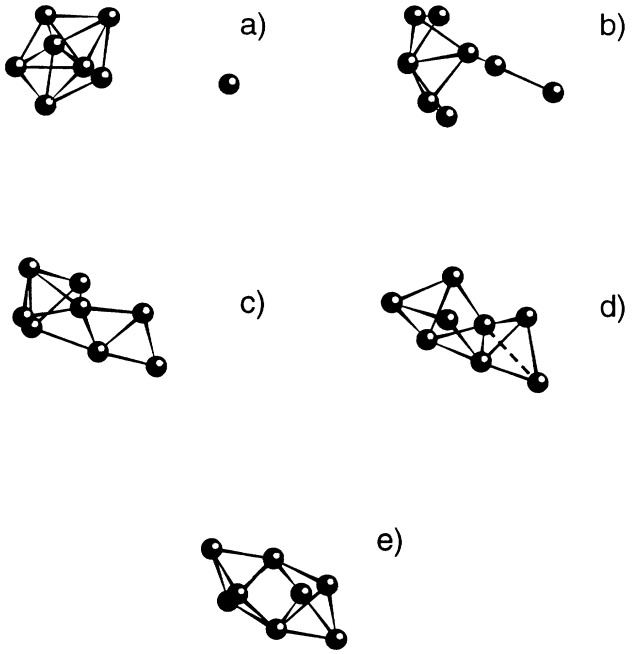


FIG. 4. Binding of an adatom to the $Si_7$ cluster at 2000 K. (a) The initial configuration, (b–d) some configurations observed during the isothermal simulation, and (e) the annealed structure are illustrated.

It is clear that by using relatively low initial simulation temperatures (1500–2000 K), the annealing corresponds to a selective type of search which can easily result in local minima. On the other hand, because the adatom simulations exploit the high symmetry of the clusters and their natural tendency to grow by face capping, or eventually edge capping, such simulations appear to be useful to generate low-energy structures at a relatively low computational cost. This type of search can always be improved by using a higher simulation temperature, since one eventually ends up reproducing a full annealing.

## V. CONCLUSIONS

We have presented an *ab initio* approach to determine the structure of complex low-symmetry atomic systems. The approach is based on Langevin molecular-dynamics and quantum-mechanical forces derived from self-consistent pseudopotential calculations. No fictitious electron dynamics is involved. As an illustrative application of the method, we have examined several clusters of $Si_n$ with $n \leq 13$. We have determined the ground state of

neutral and of some charged species of these clusters, and exploited the Langevin constant-temperature simulation approach to examine a simple adsorption process.

The random forces in Langevin molecular dynamics are useful for eliminating kinetic barriers and "shaking" ions out of metastable states. However, their effect on the evolution of the electronic states, if not decoupled from the ionic motion, is undesirable, and could even be counterproductive. It is not clear that a Car-Parrinello approach based on fictitious electron dynamics is appropriate for implementation into a Langevin molecular-dynamics procedure. Moreover, we find the numerical effort in self-consistently solving the Kohn-Sham equations at each time step by iterative diagonalizations to be comparable[37] to the effort involved with a Car-Parrinello simulation.

One advantage of the Langevin approach is that it can be used to simulate properties as a function of temperature. It is an ideal tool to examine the properties of clusters in a buffer gas, as the random fluctuation and dissipative forces have a physical analogy in the collision and dissipative effects with gas molecules. The method can also be used in the simulation of surfaces, or the deposition of atoms on surfaces. A temperature gradient perpendicular to the surface can be easily introduced by means of the fluctuating forces. Such a procedure may be useful to simulate crystal growth.

## ACKNOWLEDGMENTS

We would like to thank J. L. Martins and N. Troullier for fruitful discussions. We acknowledge support for this work by the National Science Foundation. One of us (N.B.) acknowledges support from the Swiss National Science Foundation under Grant No. 20-39528.93. We would also like to acknowledge computational support from the Minnesota Supercomputer Institute.

## APPENDIX

The generalized Langevin equation reads[18]

$$\frac{dy_j}{dt}=m_j(\vec{y})+\sum_{k=1}^{N}\sigma_{jk}g_k(t)\ , \tag{A1}$$

where $\vec{y}=(y_1,\ldots,y_N)$ is a set of variables characterizing the state of the system, $\vec{m}=(m_1,\ldots,m_N)$ a set of deterministic external forces, and $\vec{g}(t)=[g_1(t),\ldots,g_N(t)]$ a set of Gaussian random forces with a white spectrum:

$$\begin{aligned}&\langle g_k(t)\rangle=0\ ,\\ &\langle g_k(t)g_j(t')\rangle=2c_{kj}\delta(t-t')\ ,\end{aligned} \tag{A2}$$

where the angular brackets denote macroscopic (ensemble or time) averages.

The transition probability, $P(\vec{y}_0,t_0|\vec{y},t)$ associated with the process described by Eq. (A1) satisfies a Fokker-Planck equation:[18]

$$\partial_t P+\mathrm{div}\vec{J}=0\ , \tag{A3}$$

where

$$\vec{J}=\vec{m}P-D\ \vec{\mathrm{grad}}P \tag{A4}$$

and where $D$ is defined by

$$D_{ij}=\sum_{kl}\sigma_{ik}\sigma_{jl}c_{kl}\ . \tag{A5}$$

The Langevin equation (1) with the conditions (2) is a special case of Eqs. (A1) and (A2) where $N$ is six times the number of particles $n_a$ in the system. This special case is obtained by setting

$$\vec{y}=(R_1^x,\ldots,R_{n_a}^z,V_1^x,\ldots,V_{n_a}^z)\ ,$$

with $\mathbf{V}_j=\dot{\mathbf{R}}_j$, and

$$\begin{aligned}\vec{m}=[&V_1^x,\ldots,V_{n_a}^z,f_1^x(\{R_i^\alpha\},\{V_i^\alpha\}),\ldots,\\ &f_{n_a}^z(\{R_i^\alpha\},\{V_i^\alpha\})]\ ,\end{aligned}$$

with

$$\mathbf{f}_j=-\nabla_{\mathbf{R}_j}E(\{R_i^\alpha\})/M_j-\gamma\mathbf{V}_j\ ,$$

and by imposing $\sigma_{ij}=c_{ij}=0$ for $i\neq j$, and $\sigma_{ii}=c_{ii}=0$ for $i\leq 3n_a$. The conditions on $c_{ij}$ and $\sigma_{ij}$ imply that the only nonvanishing elements of $D$ are

$$\{D_{jj}\}_{j>3n_a}\equiv\{d_i^\alpha\}_{i=1,n_a}^{\alpha=x,y,z}\ .$$

The Langevin equation is often referred to as the Kramer equation when the components of $\vec{y}$ are the position and velocity.

We are interested here in the long-time behavior of the transition probability for a Langevin process described by Eqs. (1) and (2) with natural boundary conditions or with periodic boundary conditions and a periodic potential. In the long-time limit, $t\rightarrow\infty$, the probability distribution is expected to be a stationary solution of the Fokker-Planck equation. The stationary solution is given by

$$\mathrm{div}\vec{J}=0\ . \tag{A6}$$

With the restrictions given above on $\vec{m}$ and $D$, which apply to Eqs. (1) and (2), one finds [by direct insertion in (A6)] that a probability distribution of the Boltzmann type,

$$P\sim\exp\left[-\beta\left[\sum_j\tfrac{1}{2}M_j|\mathbf{V}_j|^2+\mathbf{E}(\{\mathbf{R}_i\})\right]\right]\ , \tag{A7}$$

is a stationary solution of the Fokker-Planck equation for $d_i^\alpha=\gamma/M_i\beta$. The latter relationship leads to the fluctuation-dissipation equation (2) when

$$\{G_i^\alpha(t)\}_{i=1,n_a}^{\alpha=x,y,z}\equiv\{\sigma_{jj}g_j(t)\}_{j=3n_a+1,N}$$

is used in Eq. (A2). One can also show that the stationary solution (A7) is unique for a process described by the Kramer equation.[18]

[1]S. Kirkpatrick, C. D. Gelatt, and M. P. Vecchi, Science **220**, 671 (1983).

[2]R. Biswas and D. R. Hamann, Phys. Rev. B **34**, 895 (1986).

[3]J. R. Chelikowsky and J. C. Phillips, Phys. Rev. B **41**, 5735 (1990); J. R. Chelikowsky, K. M. Glassford, and J. C. Phillips, *ibid.* **44**, 1538 (1991).

[4]J. R. Chelikowsky, Phys. Rev. Lett. **67**, 2970 (1991).

[5]R. Car and M. Parrinello, Phys. Rev. Lett. **55**, 2471 (1985).

[6]D. Hohl, R. O. Jones, R. Car, and M. Parrinello, Phys. Rev. Lett. **55**, 2471 (1985); J. Chem. Phys. **89**, 6823 (1988).

[7]P. Ballone and W. Andreoni, Phys. Rev. Lett. **60**, 271 (1988); R. Car, M. Parrinello, and W. Andreoni, in *Microclusters*, edited by S. Sugano, Y. Nishina, and S. Ohnishi, Springer Series in Materials Science Vol. 4 (Springer-Verlag, Berlin, 1987), p. 134; P. Ballone, W. Andreoni, R. Car, and M. Parrinello, Europhys. Lett. **8**, 73 (1989); U. Rötlisberg, W. Andreoni, and M. Parrinello, Phys. Rev. Lett. **72**, 665 (1994).

[8]R. Kawai and J. H. Weare, Phys. Rev. Lett. **65**, 80 (1990).

[9]J.-Y. Yi, D. J. Oh, and J. Bernholc, Phys. Rev. Lett. **67**, 1594 (1991).

[10]V. Kumar and R. Car, Phys. Rev. B **44**, 8243 (1991).

[11]U. Rötlisberg, W. Andreoni, and P. Giannozzi, J. Chem. Phys. **96**, 1248 (1991).

[12]R. M. Wentzcovitch and J. L. Martins, Solid State Commun. **78**, 831 (1991).

[13]T. A. Arias, M. C. Payne, and J. D. Joannopoulos, Phys. Rev. B **45**, 1538 (1992).

[14]N. Binggeli, J. L. Martins, and J. R. Chelikowsky, Phys. Rev. Lett. **68**, 2956 (1992), present a preliminary version of this work.

[15]Simulated annealing with the Car-Parrinello method could, in principle, be performed without the adiabatic constraint and using larger time steps. This, however, may not necessarily lead to a faster annealing, especially in the case of metallic systems, in which charge oscillation is normally a problem.

[16]M. F. Jarrold, Science **252**, 1085 (1991); M. F. Jarrold and V. A. Constant, Phys. Rev. Lett. **67**, 2994 (1991).

[17]R. Kubo, Rep. Prog. Theor. Phys. **29**, 255 (1966).

[18]H. Risken, *The Fokker-Planck Equation* (Springer-Verlag, Berlin, 1984); R. L. Stratanovitch, *Topics in the Theory of Random Noise* (Gordon and Breach, New York, 1967); N. G. Van Kampen, *Stochastic Processes in Physics and Chemistry* (North-Holland, Amsterdam, 1981).

[19]To generate a canonical distribution, $P=\exp[-E(\{R_j\})/k_BT]$, in coordinate space, a Langevin equation of the type $\dot{R}_j=-\partial_{R_j}E(\{R_j\})+G_j(t)$, where $G_j$ are Gaussians random variables with a white spectrum: $\langle G_j(t)\rangle=0, \langle G_i(t)G_j(t')\rangle=2k_BT\delta_{ij}\delta(t-t')$, could be used. This approach would correspond to the high viscosity limit of Eq. (1).

[20]S. Nosé, Mol. Phys. **52**, 255 (1984); W. G. Hoover, Phys. Rev. A **31**, 1695 (1985).

[21]J. L. Martins and M. L. Cohen, Phys. Rev. B **37**, 6134 (1988).

[22]C. G. Broyen, Math. Comput. **19**, 577 (1965).

[23]C. L. Fu and K. M. Ho, Phys. Rev. B **28**, 5480 (1983).

[24]S. de Gironcoli, P. Giannozzi, and A. Baldereschi (unpublished).

[25]For the quantum-mechanical forces, the terms relative to the single orbital contributions are simply weighted by the electronic level occupation number. This procedure insures a proper variational scheme for total energies computed with the Gaussian broadening technique. See also Ref. 24.

[26]This approach has been used to study charged impurities, see, e.g., C.G. van de Walle, P. J. H. Denteneer, Y. Bar-Yam, and S. T. Pantelides, Phys. Rev. B **39**, 10 791 (1989); S. Froyen and A. Zunger, *ibid.* **34**, 7451 (1986).

[27]N. Troullier and J. L. Martins, Phys. Rev. B **43**, 1993 (1991); **43**, 8861 (1993).

[28]L. Kleinman and D. M. Bylander, Phys. Rev. Lett. **48**, 1425 (1982).

[29]D. M. Ceperley and B. J. Alder, Phys. Rev. Lett. **45**, 566 (1980).

[30]J. P. Perdew and A. Zunger, Phys. Rev. B **23**, 5048 (1981).

[31]J. C. Tully, G. H. Gilmer, and M. Shugard, J. Chem. Phys. **71**, 1630 (1979).

[32]K. Raghavachari and V. Logovinsky, Phys. Rev. Lett. **55**, 2853 (1985).

[33]K. Raghavachari, J. Chem. Phys. **84**, 5673 (1986); Phase Transitions **24-26**, 61 (1990).

[34]K. Raghavachari and C. M. Rohlfing, J. Chem. Phys. **94**, 3670 (1990).

[35]J. C. Phillips, Phys. Rev. B **47**, 14 132 (1993).

[36]E. C. Honea, A. Ogura, C. A. Murray, K. Raghavachari, W. O. Sprenger, M. F. Jarrold, and W. L. Brown, Nature **366**, 42 (1993).

[37]For $Si_{13}$, a total of about 150 matrix-vector multiplications per eigenstate were performed at each LMD time step for diagonalization and self-consistency. Our time step is about 60 times larger than in the Car-Parrinello simulation for $Si_{10}$ in which a single matrix operation per electronic state is performed at each step. Thus, the computation burden as measured by the number of matrix multiplications per LMD time period is comparable.